SCIENTIFIC REPORTS
natureresearch

OPEN

Extracorporeal Life Support Enhances the Forward Pressure Wave to Cause a Mismatch between Cardiac Oxygen Demand and Supply

Chih-Hsien Wang[1], Ru-Wen Chang[1], En-Ting Wu[2], Yi-Jing Hsiao[3], Ming-Shiou Wu[4], Hsi-Yu Yu[1], Yih-Sharng Chen[1], Liang-Chuan Lai[5] & Sung-Liang Yu[3]

Extracorporeal life support (ECLS) is a world-famous life-saving method. Until now, changes in arterial wave properties due to ECLS have remained unexamined. In this study, we determined the effects of ECLS on arterial wave properties and ventricular/arterial coupling in male Wistar rats with the measured aortic pressure alone. Ascending aortic pressure signals were measured before ECLS and at 30, 60, and 90 min after weaned off. The aortic pressure signal then calculated by fourth-order derivative to obtain an assumed triangular flow wave. The ratio of mean systolic pressure to mean diastolic pressure (P_{ms}/P_{md}), a parameter for evaluating the matching condition between myocardial oxygen demand and supply, was significantly higher after ECLS. The magnitude of forward pressure ($|P_f|$) augmented by ECLS prevailed over the backward pressure ($|P_b|$), leading to a decline in wave reflection factor. P_{ms}/P_{md} was positively linearly correlated with $|P_f|$ ($P_{ms}/P_{md} = 0.9177 + 0.0078 \times |P_f|$, $r = 0.8677$; $P < 0.0001$). These findings suggest that $|P_f|$ was a predominant factor responsible for the mismatch between the myocardial oxygen demand and supply in rats after ECLS phase of experiment.

Extracorporeal life support (ECLS) has become a life-saving method for adults[1,2] and children[3,4] worldwide since its first successful use in 1971[5]. The implementation usually involves femoral cannulation due to its simplicity, efficiency, and ease of use outside the operating room[6]. Although the success rates of ECLS have improved, it still causes some severe side effects. Reports from clinical investigations have indicated that management with ECLS might induce significant complications, such as acute kidney injury[7], bleeding[8], and inflammatory insults[8]. Moreover, femoral cannulation causes massive retrograde aortic ECLS flow[6,9], causing a watershed of the cardiac and ECLS flows in the aortic arch during ECLS[9]. Whether the massive retrograde aortic ECLS flow might exert deteriorative effects on arterial wave properties and matching condition of oxygen demand and supply in myocardium has not been investigated until now.

The accurate measurement of the pulsatile nature of the arterial system, including arterial wave transit time (τ_w) and the forward (P_f) and backward (P_b) pressure waves, requires simultaneous recording of aortic pressure and flow signals[10–12]. However, it is difficult to steadily measure the ascending aortic flow signal in rats and humans before, during, and after ECLS. In 2006, Westerhof et al.[13] described and validated that the aortic flow can be approximated by a triangle (Q^{tri}), which is constructed from the measured aortic pressure waveform. Based on aortic pressure and Q^{tri}, P_f and P_b, components of aortic pressure wave, were successfully obtained by the wave separation method. Moreover, Chang et al.[14] discovered that the aortic impulse response is effective for estimating arterial τ_w by a single pressure pulse with its corresponding Q^{tri}. The novelty of the concept proposed

[1]Cardiovascular Surgery, Department of Surgery, National Taiwan University Hospital, Taipei, Taiwan. [2]Department of Pediatrics, College of Medicine, National Taiwan University Hospital, Taipei, Taiwan. [3]Department of Clinical and Laboratory Sciences and Medical Biotechnology, National Taiwan University College of Medicine, Taipei, Taiwan. [4]Department of Internal Medicine, National Taiwan University Hospital, Taipei, Taiwan. [5]Department of Physiology, College of Medicine, National Taiwan University, Taipei, Taiwan. Correspondence and requests for materials should be addressed to C.-H.W. (email: wchemail@gmail.com or wchemail@ntu.edu.tw)

	HR	CL	LVET	P_s	P_d	P_m	PP
Time point							
Baseline	366.5 ± 27.1	163.7 ± 12.5	60.6 ± 5.2	113.0 ± 20.4	80.8 ± 20.6	98.3 ± 19.7	31.7 ± 7.2
Post-ECLS 30 min	390.8 ± 22.2*	153.5 ± 8.8*	56.4 ± 6.1*	123.6 ± 18.2	79.4 ± 30.5	100.7 ± 33.1	44.4 ± 12.5*
Post-ECLS 60 min	398.4 ± 33.8*	150.6 ± 12.7*	53.7 ± 5.8*	122.8 ± 18.9	79.9 ± 23.6	100.9 ± 24.1	43.1 ± 15.0*
Post-ECLS 90 min	394.9 ± 49.3*	151.9 ± 18.5*	53.3 ± 7.0*	122.9 ± 22.0	81.2 ± 31.0	104.1 ± 31.0	42.4 ± 14.6*†#

Table 1. Basic hemodynamic data measured in rats at baseline and at 30, 60, and 90 min post-ECLS. Variables are expressed as median ± interquartile range (IQR). HR = heart rate (beats min^{-1}); CL = cardiac cycle length (ms, which means the duration of single beat); LVET = left ventricular ejection time (ms, which was derived from the duration of the first two vertical lines in Fig. 1A–D); P_s = systolic pressure (mmHg); P_d = diastolic pressure (mmHg); P_m = mean pressure (mmHg); PP = pulse pressure (mmHg). *$P < 0.05$ compared with baseline. †$P < 0.05$ compared with post-ECLS 30 min. #$P < 0.05$ compared with post-ECLS 60 min.

by Westerhof et al. is that the constructed Q^{tri}, approximately to its paired flow signal, is based on the measured aortic pressure wave, and the calibration is not required in the analysis[13].

Ventricular/arterial coupling concerns two matters, action of the heart as a pump connected to a hydraulic load and perfusion of the heart as an organ. In 1972, Buckberg et al.[15] showed that an index based on LV and aortic pressures could predict subendocardial ischemia: the area between the diastolic aortic and LV pressures (DPTI) represented the oxygen supply to the myocardium, and the area under the systolic LV pressure curve (SPTI) represented the oxygen demand by the myocardium. As pressure in the ventricle during systole is approximated by aortic pressure during systole, for practical purpose, O'Rourke[10] and O'Rourke et al.[16] suggested that ventricular function as pumping action could be described using mean pressure generated in the ascending aorta during systole. Thus, the ratio of mean systolic aortic pressure (P_{ms}) to the mean diastolic aortic pressure (P_{md}) could be an indicator for evaluating the matching condition between myocardial oxygen demand and supply.

In this study, we used the measured aortic pressure and an assumed Q^{tri} to determine the effects of ECLS on arterial wave properties and ventricular/arterial coupling in male Wistar rats. The construction of Q^{tri} was derived from the fourth-order derivative of the measured aortic pressure wave[13,14,17]. The aortic input impedance (Z_i) was calculated from the ratio of the ascending aortic pressure harmonics to the corresponding Q^{tri} harmonics. The arterial τ_w was determined by the aortic impulse response, which is the time-domain equivalent of its Z_i in the frequency-domain. The P_f and P_b components of the pressure pulse were separated using the wave decomposition technique. Thus, the arterial τ_w, and magnitudes of the forward ($|P_f|$) and backward ($|P_b|$) pressure waves were derived from the only measured aortic pressure to delineate the changes caused by ECLS in the pulsatile nature of the LV afterload.

Results

Hemodynamic parameters compared between baseline and post-ECLS 30, 60, 90 min.
The mean body weight of the rats was 500 ± 35 g. Table 1 shows the basal heart rate (HR), cardiac cycle length (CL), LV ejection time (LVET), and aortic pressure profiles before and after ECLS treatment. After weaning from ECLS, the rats had increased HR, decreased CL, and shortened LVET. By contrast, no significant difference was observed in these parameters between post-ECLS 30, 60, and 90 min. The systolic (P_s), diastolic (P_d), and mean (P_m) aortic blood pressures did not change significantly in these rats after ECLS. By contrast, the PP values were markedly higher at post-ECLS 30, 60, and 90 min than at baseline.

Table 2 shows the mean systolic (P_{ms}), and mean diastolic (P_{md}) aortic blood pressures and the fold changes compared with its baseline. They did not change significantly after ECLS. However, the P_{ms}/P_{md} ratio significantly increased following ECLS and markedly decreased at post-ECLS 60 and 90 min compared with 30 min.

Pulse wave reflection changed by ECLS.
Table 3 shows the pulse wave reflection obtained from the aortic pulsatile pressure signal in rats before and after ECLS. After ECLS, the rats had significantly higher $|P_f|$ and $|P_b|$ than before ECLS. The fold changes of $|P_f|$ and $|P_b|$ also significantly increased after ECLS, with the fold change level of $|P_f|$ being higher than that of $|P_b|$. Although there was a trend toward decreasing arterial τ_w in rats following ECLS, the τ_w/CL ratio remained unaltered.

The constructed Q^{tri} derived from the measure pressure wave in one rat.
Figure 1 shows the construction of an uncalibrated Q^{tri} obtained from the measured pressure wave in a rat at baseline (A) and at 30 (B), 60 (C), and 90 (D) min post-ECLS. The aortic pressure wave was measured from the ascending aorta under anesthesia and in the closed-chest condition. Aortic impulse response function curve (Fig. 1E–H) obtained from the measured aortic pressure with its paired Q^{tri}. In I-L, the amplitudes (peak – trough) of the P_f and P_b are represented by $|P_f|$ and $|P_b|$, respectively.

P_f dominated the increase in P_{ms}/P_{md} ratio, which can also be easily detected by PP, after ECLS.
Figure 2 illustrates the performance of ECLS on the arterial wave properties including RM, RI, and τ_w/LVET ratio. The RM (Fig. 2A) and RI (Fig. 2B) values at baseline were significantly higher than at post-ECLS 30, 60, and 90 min. By contrast, the τ_w/LVET ratio did not significantly change before and after ECLS (Fig. 2C).

Figure 3 shows the prediction of P_{ms}/P_{md} ratio from the τ_w/LVET ratio and RI before and after ECLS. Taking P_{ms}/P_{md} as the dependent variable and arterial τ_w/LVET and RI as independent variables, multiple linear
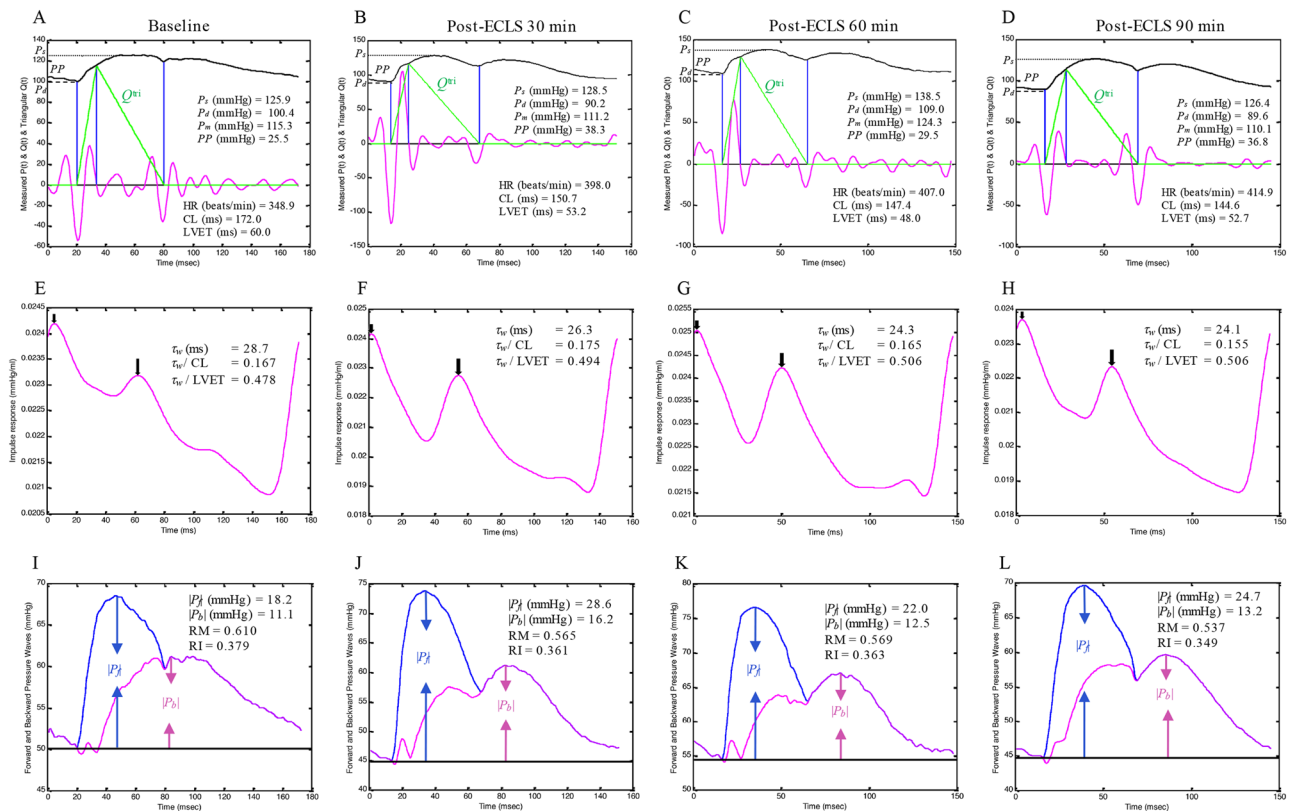
Figure 1. Construction of an uncalibrated Q^{tri} derived from the measured pressure waveform in a rat at baseline (**A**) and at 30 (**B**), 60 (**C**), and 90 (**D**) min post-ECLS. In (**E–H**), the aortic impulse response function curve derived from the measured aortic pressure and its assumed Q^{tri}. In (**I–L**), the amplitudes (peak – trough) of the P_f and P_b are described by $|P_f|$ and $|P_b|$, respectively. CL = cardiac cycle length; HR = basal heart rate; LVET = left ventricular ejection time; P_b = backward pressure wave; P_d = diastolic pressure; P_f = forward pressure wave; P_m = mean aortic pressure; P_s = systolic pressure; PP = pulse pressure; Q^{tri} = triangular flow; RM = wave reflection magnitude, given by $|P_b|/|P_f|$; RI = wave reflection index, given by $|P_b|/(|P_f| + |P_b|)$; τ_w = wave transit time.

	P_{ms}	Fold change	P_{md}	Fold change	P_{ms}/P_{md}
Time point					
Baseline	106.0 ± 19.7	1.000 ± 0.000	93.5 ± 20.8	1.000 ± 0.000	1.114 ± 0.058
Post-ECLS 30 min	110.2 ± 29.3	1.063 ± 0.219	91.3 ± 34.0	0.949 ± 0.383	$1.169 \pm 0.118^{*}$
Post-ECLS 60 min	110.2 ± 21.0	1.064 ± 0.227	95.9 ± 25.1	1.038 ± 0.343	$1.157 \pm 0.104^{*\dagger}$
Post-ECLS 90 min	113.7 ± 26.5	1.105 ± 0.205	95.6 ± 32.1	1.003 ± 0.400	$1.155 \pm 0.101^{*\dagger}$

Table 2. Effects of ECLS on the mean systolic and the mean diastolic pressure in rats at baseline and at 30, 60, and 90 min post-ECLS. Variables are expressed as median ± interquartile range (IQR). P_{ms} = mean systolic pressure (mmHg); P_{md} = mean diastolic pressure (mmHg). *$P < 0.05$ compared with baseline. †$P < 0.05$ compared with post-ECLS 30 min.

regression was employed to fit the data. Only the correlation between P_{ms}/P_{md} and RI reached significance. The influences of $|P_f|$ and $|P_b|$ on P_{ms}/P_{md} ratio are depicted in Fig. 4A. The correlation between P_{ms}/P_{md} and $|P_f|$ (but not $|P_b|$) achieved significance. Figure 4B shows the positive linear relationship between the P_{ms}/P_{md} and $|P_f|$ in rats before and after ECLS ($P_{ms}/P_{md} = 0.9177 + 0.0078 \times |P_f|$ ($r = 0.8677$; $P < 0.0001$).

Figure 5 displays the relationship of P_{ms}/P_{md} ratio and PP in rats before and after ECLS. PP had a significantly positive regression with P_{ms}/P_{md}: $P_{ms}/P_{md} = 0.8716 + 0.0074 \times PP$ ($r = 0.9059$; $P < 0.0001$).

Discussion

Although ECLS can be used as a bridge to recovery for patients with severe heart failure[18] or heart transplantation[19], this technology is associated with several side effects, such as blood cell consumption and activation of the cytokine network and the complement cascade systems[20,21]. Theoretically, retrograde aortic ECLS flow can increase cardiac afterload, thus leading to LV distension and endangering ventricular recovery[9]. However, little

	$|P_f|$	Fold change	$|P_b|$	Fold change	τ_w	τ_w/CL
Time point						
Baseline	22.5 ± 6.7	1.000 ± 0.000	12.4 ± 2.1	1.000 ± 0.000	30.1 ± 3.0	0.180 ± 0.016
Post-ECLS 30 min	$32.5 \pm 14.5^*$	$1.594 \pm 0.505^*$	$16.0 \pm 2.2^*$	$1.326 \pm 0.248^*$	26.7 ± 2.6	0.178 ± 0.020
Post-ECLS 60 min	$33.8 \pm 15.7^*$	$1.611 \pm 0.395^*$	$15.7 \pm 2.2^*$	$1.232 \pm 0.210^*$	26.5 ± 3.0	0.182 ± 0.022
Post-ECLS 90 min	$31.7 \pm 14.0^*$	$1.467 \pm 0.497^*$	$14.9 \pm 2.7^*$	$1.208 \pm 0.231^*$	26.6 ± 3.0	0.180 ± 0.022

Table 3. Effects of ECLS on the pulse wave reflection obtained from aortic pressure waveform in rats at baseline and at 30, 60, and 90 min post-ECLS. Variables are expressed as median $\pm$ interquartile range (IQR). CL = cardiac cycle length (ms); $|P_f|$ = magnitude of forward pressure wave (mmHg); $|P_b|$ = magnitude of reflected pressure wave (mmHg); τ_w = arterial wave transit time (ms). $^*P < 0.05$ compared with baseline.

attention has been given to the pulsatile hemodynamic response to ECLS, which disrupts the ventricular/arterial coupling. To the best of our knowledge, this is the first study suggesting that ECLS can enhance $|P_f|$, the predominant factor responsible for the mismatch between the myocardial oxygen demand and supply.

In this study, the rats exhibited increased HR and shortened LVET after ECLS. We had previously observed high levels of inflammatory cytokines in rats at 120 min after reperfusion[22], demonstrating persistent inflammatory insults, even after the rats had been weaned from ECLS. These inflammatory responses can be induced by the adrenergic pro-inflammatory pathway[23], which might cause accelerated heartbeat after ECLS[22]. However, ECLS exerted no significant alterations in aortic pressure profiles such as P_s, P_d, P_m, P_{ms}, and P_{md} except PP and P_{ms}/P_{md}.

The arterial τ_w can be determined by the pulse wave velocity (PWV) and traveling distance of pressure waves to the reflecting site[24]. In this study, we calculated the arterial τ_w using the aortic impulse response, which presented the two discrete reflection peaks respectively linked to the effective reflection sites (Fig. 1E–H)[25]. Since CL was a factor influencing the calculation of arterial τ_w, the τ_w/CL ratio was derived as an index for the description of aortic stiffness. Neither arterial τ_w nor τ_w/CL changed significantly after the rats had been weaned from ECLS, indicating that ECLS did not alter vasculature distensibility. Moreover, the return time of $|P_b|$ occurred during diastole in rats before and after ECLS (Fig. 1I–L). Both $|P_f|$ and $|P_b|$ were increased by ECLS (Table 3). However, the predominant role in increasing $|P_f|$ rather than $|P_b|$ contributed to a decline in RM (Fig. 2A) and RI (Fig. 2B). Although controversial, the prevalent view considers that the $|P_f|$ value primarily reveals the interaction between peak aortic flow and proximal aortic diameter/stiffness while minimal/delayed reflections occur[26–28]. Thus, the increased $|P_f|$ in the absence of changes in both τ_w and τ_w/CL indicated that ECLS may cause a functional mismatch between peak flow and physical properties of the proximal aortas.

The LV-arterial system interaction is an essential determinant of cardiovascular function and plays a crucial role in various cardiovascular disease states. Scholars have expressed great interest in characterizing the LV-arterial coupling by only measuring the ascending aortic pressure. Since coronary flow to the LV wall can occur only during diastole, the coronary perfusion pressure is the pressure gradient between the aorta and the LV during diastole, when the myocardium receives oxygen. However, the pressure generated by the left ventricle during systole is the pressure that opposes ejection of blood from the ventricle, and that determines myocardial oxygen requirements[29]. As mentioned previously, O'Rourke et al.[16] suggested that the ascending aortic pressure wave comprises two components: P_{ms}, describing the LV performance as a pump, and P_{md}, relating to LV perfusion. Depending on this, the "ideal" ventricular/arterial coupling for adequate organ flow needs to meet as low a P_{ms} and as high a P_{md} as possible. Low P_{ms} allows adequate ventricular ejection with low oxygen demands by myocardium and high P_{md} allows adequate coronary perfusion. Therefore, the increased P_{ms}/P_{md} ratio may cause a mismatch of the oxygen demand and supply in myocardium. In the present study, the rats after ECLS had higher P_{ms}/P_{md} ratio than before (Table 2). Because the pulsatile nature of LV afterload could influence the LV function, we investigated the association of P_{ms}/P_{md} with τ_w/LVET and RI by using multiple linear regression analysis. We found that P_{ms}/P_{md} was significantly affected by the magnitude of RI rather than the wave transmission time (τ_w/LVET) (Fig. 3). Because $|P_f|$ and $|P_b|$ are the determinants of RI, the multiple linear regression analysis was performed to determine the influences of $|P_f|$ and $|P_b|$ on the P_{ms}/P_{md} ratio. We identified a positive linear correlation between the P_{ms}/P_{md} and $|P_f|$ (Fig. 4), indicating that the increased $|P_f|$ by ECLS impaired the matching condition of oxygen demand and supply in myocardium.

In the present study, the PP value was markedly larger after ECLS than before (Table 1). It has been considered that increased PWV, associated with vascular stiffening, and the consequent earlier return of reflected waves, prominently contribute to elevated PP[24,30,31]. However, we found that ECLS caused a decline in RM and RI, with no alteration in arterial τ_w and τ_w/CL. Recent reports from Framingham investigators have demonstrated that increased $|P_f|$ is the predominant contributor to elevated PP with aging, with only modest contributions from wave reflections[26–28]. Thus, increased $|P_f|$ may be the predominant factor responsible for the elevated PP in rats after ECLS, with little alteration in wave transit time and a decline in wave reflection factor. The P_{ms}/P_{md} ratio surged by ECLS was positively relevant to aortic PP (Fig. 5), indicating that the increased PP by ECLS impaired the matching condition of oxygen demand and supply in myocardium.

This study has some limitations. Because a rat's blood volume is approximately 7% of that rat's body weight[32], the priming volume of our extracorporeal membrane oxygenator (ECMO) circuit was about 19–20 ml, which accounted for 61% of blood volume in the studied rats[22]. The priming volume used in this study was the minimum volume that we could attain in our model. As Z_i cannot be measured in conscious animals, it is difficult to evaluate the effects of anesthesia on the pulsatile hemodynamics in rats. The results reported here, therefore, pertain only to the measurements made in anesthetized rats. This condition might have induced changes in the aortic
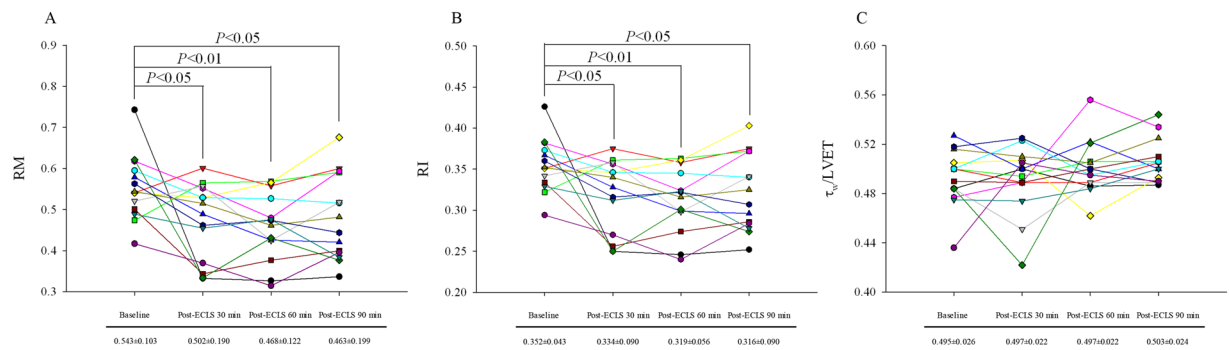
Figure 2. Effects of ECLS on the changes of RM (**A**), RI (**B**), and τ_w/LVET (**C**). Each line represents a different rat in this study. RM and RI show downward trends, which decreased markedly after ECLS treatment. The τ_w/LVET ratio tended to slightly increase after ECLS treatment. RI = wave reflection index; RM = wave reflection magnitude; τ_w/LVET = the ratio of wave transit time to left ventricular ejection period.
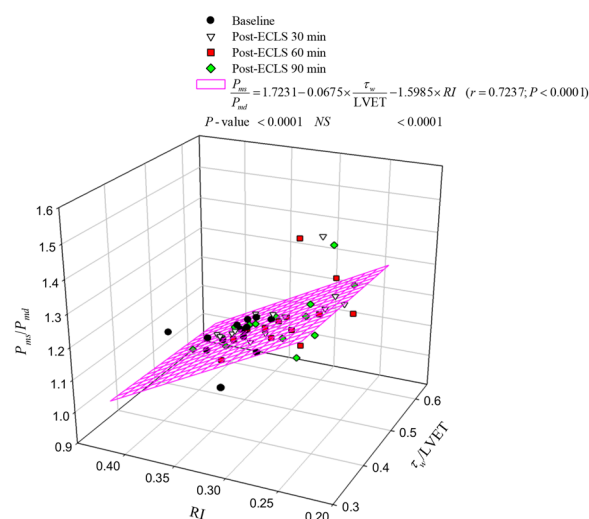

Figure 3. Implication of τ_w/LVET and RI in P_{ms}/P_{md} ratio in rats before and after ECLS. As shown by multiple linear regression analysis, only the correlation between P_{ms}/P_{md} and RI reached significance, suggesting that the P_{ms}/P_{md} impaired by ECLS could be affected by the magnitude of RI rather than the wave transmission time (τ_w/LVET). P_{md} = mean diastolic pressure; P_{ms} = mean systolic pressure; RI = wave reflection index; τ_w/LVET = the ratio of wave transit time to left ventricular ejection period.

pressure profiles and introduced reflex effects not observed under ordinary conditions. The degree to which anesthesia influences the pulsatile hemodynamics in rats remains unclear. However, studies with other animal models suggest that the biological and experimental variability amid animals were small enough to neglect[33]. Moreover, the Q^{tri} was constructed by the measured aortic pressure wave to its assumed pairing flow signal. Although the approximated Q^{tri} may differ from the actual flow waveform, the use of this concept describing the arterial wave properties has been validated by Westerhof *et al.*[13] and Chang *et al.*[17].

Conclusions

We demonstrated the mechanical defects of the vasculature in rats receiving ECLS based on the measured ascending aortic pressure and an assumed triangular flow. Although RI was diminished by ECLS, there existed a negative linear correlation between P_{ms}/P_{md} and RI. In advance, we identified a positive linear correlation between P_{ms}/P_{md} and $|P_f|$, indicating that the increased $|P_f|$ by ECLS impaired the LV-arterial coupling. The P_{ms}/P_{md} value was also positively associated with aortic PP, indicating that the increased PP by ECLS caused a mismatch of oxygen demand and supply in myocardium. All these findings suggest that $|P_f|$ was a predominant factor responsible for the impaired oxygen demand/supply ratio in the rats after ECLS. The advantage of this study is that an unknown Q^{tri} can obtain from the measured aortic pressure and the calibration of the flow is not necessary. Thus, it would provide a path to evaluate the arterial wave properties in the future clinical settings.
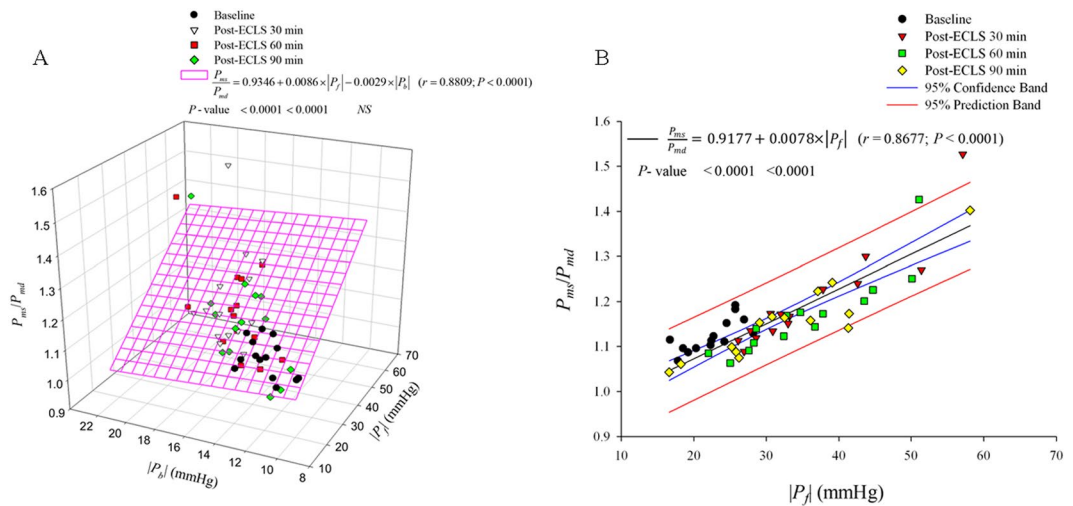
Figure 4. $|P_f|$ but not $|P_b|$ strongly correlated with P_{ms}/P_{md} in rats before and after ECLS. As shown by multiple linear regression analysis, the correlation between P_{ms}/P_{md} and $|P_f|$ and $|P_b|$ reached significance. (**A**) However, only $|P_f|$ was significantly positively related to P_{ms}/P_{md} before and after ECLS (**B**), indicating that the P_{ms}/P_{md} impaired by ECLS might be influenced by $|P_f|$ rather than $|P_b|$. P_b = backward pressure wave; P_f = forward pressure wave; P_{md} = mean diastolic pressure; P_{ms} = mean systolic pressure.
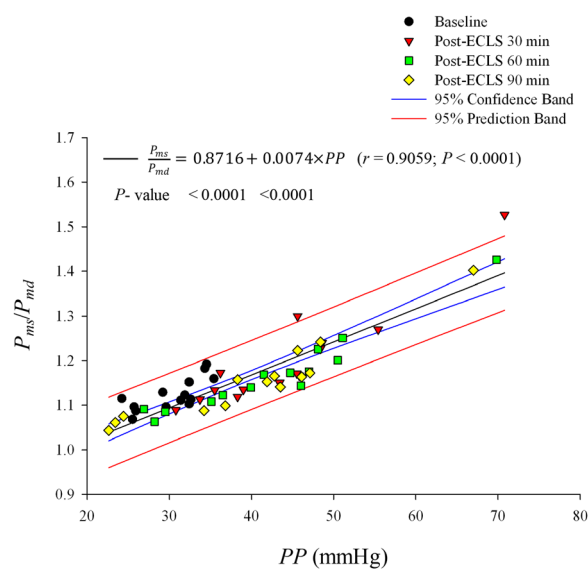
Figure 5. Potential role of PP in reflecting P_{ms}/P_{md} in rats before and after ECLS. P_{ms}/P_{md} was significantly positively related to PP by ECLS. P_{md} = mean diastolic pressure; P_{ms} = mean systolic pressure; PP = pulse pressure.

Materials and Methods

Animals and surgical procedure. The effects of ECLS on the pulsatile nature of the arterial system were evaluated in normal Wistar–Kyoto male rats weighing 450–550 g (NC + ECLS; $n = 14$). All rats were free access to Purina rat chow and water and housed two per cage in a 12-h light/dark cycle animal room. Periodic checks of the cages and body weights ensured that the food was appropriately administered. The experiment was conducted according to the *Guide for the Care and Use of Laboratory Animals*, and our study protocol was approved by the Animal Care and Use Committee of National Taiwan University.

The procedure for the implementation of ECMO in rats was conducted as described previously[22]. In brief, rats were anesthetized with 5% isoflurane/100% oxygen in an induction chamber (Serial number 4468, NorVap, Skipton, UK; Panion & BF Biotech Inc., Nangang Dist., Taipei, Taiwan), and then mechanically ventilated (tidal volume 7 mL kg^{-1}, rate 40 breaths min^{-1}, positive end-expiratory pressure 2 cmH$_2$O; Model 131, New England Medical Instruments, Medway, MA, USA) by orotracheal intubation with 1.75%–2% isoflurane/0.7–0.8 L min^{-1} oxygen for maintenance. The rats were placed on a circulating warm water blanket (B401H, Firstek Scientific Co. Ltd., Xinzhuang Dist, New Taipei City, Taiwan; TP22G, Gaymar Industries, Inc., Orchard Park, NY, 14127 USA) with a heating lamp above for maintaining body temperature[22].

The left femoral artery and vein were separately cannulated for arterial pressure monitoring (BIOPAC systems, Inc., Goleta, CA, USA) and drug administration[22]. The right femoral artery and the right external jugular vein were cannulated for the arterial inflow and venous outflow ports. Afterwards, heparin (500 UI) was administered to prevent blood clotting[22]. A high-fidelity pressure catheter (model SPC 320, size 2 French; Millar Instruments, Houston, TX, USA) was used to measure the pulsatile ascending aortic pressure from the isolated carotid artery of the right side. The electrocardiogram (ECG) of lead II was recorded using a Gould ECG/Biotech amplifier (Gould Electronics, Cleveland, OH, USA)[34]. Selective aortic pressure signals from 5 to 10 beats were averaged in the time domain, using the peak R wave of the ECG as a fiducial point[17]. Ascending aortic pressure signals were recorded in the anesthetized rats as a baseline before ECLS.

Initiation and discontinuation of ECMO and intensive care unit phase.
The ECMO device designed for rats consisted of an open venous reservoir (TERUMOR, Tokyo, Japan; 5-mL syringe), a membrane oxygenator (Micro-1 Rat Oxygenator; Dongguan Kewei Medical Instrument Co., Ltd, Guangdong, China), a heat exchanger (Radnoti Glass Technology Inc., Monrovia, CA, USA), silicone tubing (ID 1.6 mm), and a roller pump (Masterflex, Barrington, IL, USA)[22]. ECLS lasted for 30 min. The ECMO rate was initially quickly increased to the peak rate of 70 mL min^{-1}—approximately the normal cardiac output in rats—and gradually decreased to approximately 20 mL min^{-1} to meet the venous outflow. In total, 12–15 mL complement fluid made from Plasma-Lyte A (Baxter, Deerfield, IL, USA) and 6% hydroxyethyl starch 130/0.4 (Voluven$R$; Fresenius Kabi, Bad Homburg, Germany) at the ratio of 1:1 was injected during ECLS to maintain the output of the circuit system.

The rats were weaned off the system after 30 min of ECLS, and the aortic pressure waves were measured at 30, 60, and 90 min after weaning (post-ECLS 30, 60, and 90 min). Blood transfusion or drugs such as bicarbonate, inotropes, or vasopressors did not perform on rats, and the rats were all humanely euthanized at the end of the experiment.

Construction of the unknown flow wave by using a triangle.
The unknown Q^{tri} was derived from the pressure waveform measured in the ascending aorta[13,14,17]. The start and end time points of LV ejection were identified as the intersection of two vertical lines near the foot of the pressure wave (the first vertical blue line in each of Fig. 1A–D) and near the incisura (the third vertical blue line in each of Fig. 1A–D), respectively[35]. The time at the peak of the triangle was derived from the fourth-order derivative of the aortic pressure wave[13,14,17] (the pink curve in each of Fig. 1A–D). After ejection commenced, the first zero-crossing curve from above to below (the second vertical blue line in each of Fig. 1A–D) determined the peak of the triangle of blood flow, which was the inflection point of the pressure wave[13,14,36]. Thus, the uncalibrated Q^{tri} was approximated by a triangular shape (the green curves in each of Fig. 1A–D) and represented the corresponding flow wave of the aortic pressure signal.

Impulse response function curve.
Z_i was obtained from the ratio of the ascending aortic pressure harmonics to the corresponding harmonics from Q^{tri} by using a standard Fourier series expansion technique[11,14,35,37]. The aortic characteristic impedance (Z_c) was calculated by averaging the high-frequency moduli of the Z_i data points from 4 to 10 harmonics. Arterial τ_w was computed using the impulse response function curve (the pink line in each of Fig. 1E–H)[38,39], which was generated using an inverse Fourier transformation of the Z_i after multiplying the first 12 harmonics by a Dolph–Chebyshev weighting function with order 24[35,40]. One-half of the time difference between the appearance of the second reflected peak (long arrow) and the initial peak (short arrow) in the impulse response curve approximates the arterial τ_w in the lower body circulation[34,38,40,41].

Arterial wave separation analysis.
The equations used to resolve the measured aortic pressure wave (P_{ao}) into its P_f and P_b components were described as follows[35,42]:

$$P_f(t) = \frac{P_{ao}(t) + Z_c \times Q^{tri}(t)}{2} \tag{1}$$

$$P_b(t) = \frac{P_{ao}(t) - Z_c \times Q^{tri}(t)}{2} \tag{2}$$

The calculations of the P_f and P_b using $Q^{tri}(t)$ are depicted in Fig. 1I–L. The amplitudes (peak − trough) of the P_b and P_f are represented by $|P_b|$ and $|P_f|$, respectively. The aortic reflection magnitude (RM) was then defined as the ratio of $|P_b|$ and $|P_f|$: RM $= |P_b|/|P_f|$[13], and the reflection index (RI) was calculated as RI $= |P_b|/(|P_f| + |P_b|)$.

Statistical analysis.
The results are expressed as median ± interquartile range (IQR). SigmaPlot 12.5 were used for statistical analysis. Wilcoxon signed-rank testing was performed to determine the statistical significance of the results between different time points for multiple comparisons of the effects of ECLS on arterial wave properties. Statistical significance was set as $P < 0.05$.

References
1. Chen, Y. S. et al. Cardiopulmonary resuscitation with assisted extracorporeal life-support versus conventional cardiopulmonary resuscitation in adults with in-hospital cardiac arrest: an observational study and propensity analysis. *Lancet* **372**, 554–561, https://doi.org/10.1016/s0140-6736(08)60958-7 (2008).
2. Shin, T. G. et al. Extracorporeal cardiopulmonary resuscitation in patients with inhospital cardiac arrest: A comparison with conventional cardiopulmonary resuscitation. *Crit Care Med* **39**, 1–7, https://doi.org/10.1097/CCM.0b013e3181feb339 (2011).
3. Huang, S. C. et al. Extracorporeal membrane oxygenation rescue for cardiopulmonary resuscitation in pediatric patients. *Critical care medicine* **36**, 1607–1613, https://doi.org/10.1097/CCM.0b013e318170b82b (2008).
4. Topjian, A. A., Nadkarni, V. M. & Berg, R. A. Cardiopulmonary resuscitation in children. *Curr Opin Crit Care* **15**, 203–208 (2009).

5. Chauhan, S. & Subin, S. Extracorporeal membrane oxygenation, an anesthesiologist's perspective: physiology and principles. *Part 1. Ann Card Anaesth* **14**, 218–229, https://doi.org/10.4103/0971-9784.84030 (2011).
6. Haneya, A. *et al.* A 5-year experience with cardiopulmonary resuscitation using extracorporeal life support in non-postcardiotomy patients with cardiac arrest. *Resuscitation* **83**, 1331–1337, https://doi.org/10.1016/j.resuscitation.2012.07.009 (2012).
7. Hsu, P. S. *et al.* Extracorporeal membrane oxygenation for refractory cardiogenic shock after cardiac surgery: predictors of early mortality and outcome from 51 adult patients. *Eur J Cardiothorac Surg* **37**, 328–333, https://doi.org/10.1016/j.ejcts.2009.07.033 (2010).
8. Loforte, A. *et al.* Peripheral extracorporeal membrane oxygenation system as salvage treatment of patients with refractory cardiogenic shock: preliminary outcome evaluation. *Artif Organs* **36**, E53–61, https://doi.org/10.1111/j.1525-1594.2011.01423.x (2012).
9. Rupprecht, L. *et al.* Cardiac decompression on extracorporeal life support: a review and discussion of the literature. *Asaio j* **59**, 547–553, https://doi.org/10.1097/MAT.0b013e3182a4b2f6 (2013).
10. O'Rourke, M. F. Vascular impedance in studies of arterial and cardiac function. *Physiol Rev* **62**, 570–623 (1982).
11. Milnor, W. R. *Hemodynamics* 2nd Edition edn, (Williams & Wilkins, 1989).
12. McDonald, D. A. *Blood flow in arteries.* 2nd Edn. edn, (Williams & Wilkins, 1974).
13. Westerhof, B. E., Guelen, I., Westerhof, N., Karemaker, J. M. & Avolio, A. Quantification of wave reflection in the human aorta from pressure alone: a proof of principle. *Hypertension* **48**, 595–601, https://doi.org/10.1161/01.hyp.0000238330.08894.17 (2006).
14. Chang, C. Y. *et al.* Defects in Vascular Mechanics Due to Aging in Rats: Studies on Arterial Wave Properties from a Single Aortic Pressure Pulse. *Front Physiol* **8**, 503, https://doi.org/10.3389/fphys.2017.00503 (2017).
15. Buckberg, G. D., Fixler, D. E., Archie, J. P. & Hoffman, J. I. Experimental subendocardial ischemia in dogs with normal coronary arteries. *Circ Res* **30**, 67–81 (1972).
16. O'Rourke, M. F., Yaginuma, T. & Avolio, A. P. Physiological and pathophysiological implications of ventricular/vascular coupling. *Ann Biomed Eng* **12**, 119–134 (1984).
17. Chang, R. W. *et al.* Determining arterial wave transit time from a single aortic pressure pulse in rats: vascular impulse response analysis. *Sci Rep* **7**, 40998, https://doi.org/10.1038/srep40998 (2017).
18. Vardi, A. *et al.* ECMO–extra corporeal membrane oxygenation as a bridge to recovery, following surgery for complex congenital cardiac anomalies, in children and neonates. *Harefuah* **142**, 583–587, 648, 647 (2003).
19. Marasco, S. F. *et al.* Extracorporeal membrane oxygenation in primary graft failure after heart transplantation. *Ann Thorac Surg* **90**, 1541–1546, https://doi.org/10.1016/j.athoracsur.2010.05.066 (2010).
20. Hirthler, M., Simoni, J. & Dickson, M. Elevated levels of endotoxin, oxygen-derived free radicals, and cytokines during extracorporeal membrane oxygenation. *J Pediatr Surg* **27**, 1199–1202 (1992).
21. Underwood, M. J. *et al.* Changes in "inflammatory" mediators and total body water during extra-corporeal membrane oxygenation (ECMO). A preliminary study. *Int J Artif Organs* **18**, 627–632 (1995).
22. Chang, R. W., Luo, C. M., Yu, H. Y., Chen, Y. S. & Wang, C. H. Investigation of the pathophysiology of cardiopulmonary bypass using rodent extracorporeal life support model. *BMC Cardiovasc Disord* **17**, 123, https://doi.org/10.1186/s12872-017-0558-6 (2017).
23. Rittirsch, D., Flierl, M. A. & Ward, P. A. Harmful molecular mechanisms in sepsis. *Nat Rev Immunol* **8**, 776–787, https://doi.org/10.1038/nri2402 (2008).
24. Nichols, W. W. *et al.* Effects of arterial stiffness, pulse wave velocity, and wave reflections on the central aortic pressure waveform. *J Clin Hypertens (Greenwich)* **10**, 295–303 (2008).
25. O'Rourke, M. F. Pressure and flow waves in systemic arteries and the anatomical design of the arterial system. *J Appl Physiol* **23**, 139–149, https://doi.org/10.1152/jappl.1967.23.2.139 (1967).
26. Torjesen, A. A. *et al.* Forward and backward wave morphology and central pressure augmentation in men and women in the Framingham Heart Study. *Hypertension* **64**, 259–265, https://doi.org/10.1161/hypertensionaha.114.03371 (2014).
27. Cooper, L. L. *et al.* Components of hemodynamic load and cardiovascular events: the Framingham Heart Study. *Circulation* **131**, 354–361, https://doi.org/10.1161/circulationaha.114.011357 (2015).
28. Mitchell, G. F. *et al.* Hemodynamic correlates of blood pressure across the adult age spectrum: noninvasive evaluation in the Framingham Heart Study. *Circulation* **122**, 1379–1386, https://doi.org/10.1161/circulationaha.109.914507 (2010).
29. Sarnoff, S. J. *et al.* Hemodynamic determinants of oxygen consumption of the heart with special reference to the tension-time index. *Am J Physiol* **192**, 148–156 (1958).
30. O'Rourke, M. F. & Nichols, W. W. Aortic diameter, aortic stiffness, and wave reflection increase with age and isolated systolic hypertension. *Hypertension* **45**, 652–658, https://doi.org/10.1161/01.HYP.0000153793.84859.b8 (2005).
31. Laurent, S. & Boutouyrie, P. Recent advances in arterial stiffness and wave reflection in human hypertension. *Hypertension* **49**, 1202–1206, https://doi.org/10.1161/hypertensionaha.106.076166 (2007).
32. Lee, H. B. & Blaufox, M. D. Blood volume in the rat. *J Nucl Med* **26**, 72–76 (1985).
33. Cox, R. H. Three-dimensional mechanics of arterial segments *in vitro*: methods. *J Appl Physiol* **36**, 381–384 (1974).
34. Wang, C. H. *et al.* Prevention of arterial stiffening by using low-dose atorvastatin in diabetes is associated with decreased malondialdehyde. *PloS one* **9**, e90471, https://doi.org/10.1371/journal.pone.0090471 (2014).
35. Chang, R. W. *et al.* Systolic aortic pressure-time area is a useful index describing arterial wave properties in rats with diabetes. *Sci Rep* **5**, 17293, https://doi.org/10.1038/srep17293 (2015).
36. Kelly, R., Hayward, C., Avolio, A. & O'Rourke, M. Noninvasive determination of age-related changes in the human arterial pulse. *Circulation* **80**, 1652–1659 (1989).
37. Nichols, W. W. & O'Rourke, M. F. *McDonald's blood flow in arteries* 6th Edition edn, (Edward Arnold, 2011).
38. Sipkema, P., Westerhof, N. & Randall, O. S. The arterial system characterised in the time domain. *Cardiovasc Res* **14**, 270–279 (1980).
39. Latson, T. W., Yin, F. C. & Hunter, W. C. In *Ventricular/vascular coupling* (ed Frank CP Yin) 334–383 (Springer-Verlag, 1987).
40. Laxminarayan, S., Sipkema, P. & Westerhof, N. Characterization of the arterial system in the time domain. *IEEE Trans Biomed Eng* **25**, 177–184, https://doi.org/10.1109/tbme.1978.326244 (1978).
41. Wu, M. S., Chang, C. Y., Chang, R. W. & Chang, K. C. Early return of augmented wave reflection impairs left ventricular relaxation in aged Fisher 344 rats. *Exp Gerontol* **47**, 680–686, https://doi.org/10.1016/j.exger.2012.06.006 (2012).
42. Murgo, J. P., Westerhof, N., Giolma, J. P. & Altobelli, S. A. Manipulation of ascending aortic pressure and flow wave reflections with the Valsalva maneuver: relationship to input impedance. *Circulation* **63**, 122–132 (1981).

Acknowledgements

Author Contributions

R.W.C. and C.H.W. developed the concept, designed study, and wrote the manuscript. R.W.C. performed the animal experiment, collected data, and performed statistical analysis. Y.J.H., M.S.W., Y.S.C., H.Y.Y., and S.L.Y. supported funding and provided advice on surgical procedure. M.S.W., Y.S.C., E.T.W., and L.C.L. participated in data interpretation. E.T.W. and C.H.W. supervised this work and critically revised the manuscript. All authors read and approved the final manuscript.

Additional Information

Competing Interests: The authors declare no competing interests.

Publisher's note Springer Nature remains neutral with regard to jurisdictional claims in published maps and institutional affiliations.